Crossed beam reaction of cyano radicals with hydrocarbon molecules. III. Chemical dynamics of vinylcyanide ($C_2H_3CN;X\,^1A'$) formation from reaction of $CN(X\,^2\Sigma^+)$ with ethylene, $C_2H_4(X\,^1A_g)$

N. Balucani,[a] O. Asvany,[b] A. H. H. Chang, S. H. Lin, Y. T. Lee, and R. I. Kaiser[c]
Institute of Atomic and Molecular Sciences, 1, Section 4, Roosevelt Rd., 107 Taipei, Taiwan, Republic of China

Y. Osamura[d]
Department of Chemistry, Rikkyo University, 3-34-1 Nishi-ikebukuro, Toshima-ku, Tokyo, 171-8501, Japan

(Received 12 April 2000; accepted 29 June 2000)

The neutral–neutral reaction of the cyano radical, $CN(X\,^2\Sigma^+)$, with ethylene, $C_2H_4(X\,^1A_g)$, has been performed in a crossed molecular beams setup at two collision energies of 15.3 and 21.0 kJ mol^{-1} to investigate the chemical reaction dynamics to form vinylcyanide, $C_2H_3CN(X\,^1A')$ under single collision conditions. Time-of-flight spectra and the laboratory angular distributions of the C_3H_3N products have been recorded at mass-to-charge ratios 53−50. Forward-convolution fitting of the data combined with *ab initio* calculations show that the reaction has no entrance barrier, is indirect (complex forming reaction dynamics), and initiated by addition of $CN(X\,^2\Sigma^+)$ to the π electron density of the olefin to give a long-lived CH_2CH_2CN intermediate. This collision complex fragments through a tight exit transition state located 16 kJ mol^{-1} above the products via H atom elimination to vinylcyanide. In a second microchannel, CH_2CH_2CN undergoes a 1,2 H shift to form a CH_3CHCN intermediate prior to a H atom emission via a loose exit transition state located only 3 kJ mol^{-1} above the separated products. The experimentally observed mild ''sideways scattering'' at lower collision energy verifies the electronic structure calculations depicting a hydrogen atom loss in both exit transition states almost parallel to the total angular momentum vector **J** and nearly perpendicular to the C_2H_3CN molecular plane. Since the reaction has no entrance barrier, is exothermic, and all the involved transition states are located well below the energy of the separated reactants, the assignment of the vinylcyanide reaction product soundly implies that the title reaction can form vinylcyanide, C_2H_3CN, as observed in the atmosphere of Saturn's moon Titan and toward dark, molecular clouds holding temperatures as low as 10 K. In strong agreement with our theoretical calculations, the formation of the C_2H_3NC isomer was not observed. © *2000 American Institute of Physics.* [S0021-9606(00)01036-9]

I. INTRODUCTION

One of the fundamental goals of reaction dynamics is to obtain the description of a reactive system through the pertinent potential energy surface and its topology. An extensive literature[1] is now available reporting experimental and theoretical investigations at the microscopic level on the bimolecular reactions of atomic species; conversely, reports on the dynamics of reactions involving polyatomic radicals are still sparse and mainly related to simple diatomic radical reactions (for instance, $OH+H_2$, $OH+CO$, $CN+D_2$).[1,2] Numerous kinetic investigations on free radical reactions have been performed since they occur commonly in nature and play a key part in a wide variety of macroscopic phenomena, such as combustion, plasma, and atmospheric chemistry. The lack of extensive investigation at the microscopic level is mostly due to the difficulty of generating these unstable species in large quantities for laboratory studies. Methods commonly used to generate radicals include photolysis, pyrolysis, gas discharges, and *in situ* chemical reactions. In our laboratory we have recently developed a pulsed supersonic cyano $CN(X\,^2\Sigma^+)$ radical beam source[3] that can be efficiently coupled to a crossed molecular beam (CMB) apparatus with mass spectrometric detection and that has permitted us to undertake a systematic study of CN radical reaction dynamics.[4–7] The advantages of the CMB technique are well known:[8] a molecular beam experiment provides a collision-free environment, the reactant beams are well defined in angle and velocity, and an extensive cooling of the radical internal degrees of freedom is achieved during the supersonic expansion. Another advantage of the technique has been revealed to be crucial: since the scientific community is chiefly interested in CN radical reactions with hydrocarbons, detection of polyatomic product molecules is an easy task when using a mass spectrometer, while laser spectroscopy application is best applied to characterization of diatomic or triatomic products.

Among cyano radical reactions, those with unsaturated

[a]Permanent address: Dipartimento di Chimica, Università di Perugia, 06123 Perugia, Italy.
[b]Also at the Department of Physics, Technical University Chemnitz, 09107 Chemnitz, Germany.
[c]Also at the Department of Physics, Technical University Chemnitz, 09107 Chemnitz, Germany and Department of Physics, National Taiwan University, Taipei, 106, Taiwan, Republic of China. Corresponding author. Electronic mail: kaiser@po.iams.sinica.edu.tw
[d]Corresponding author. Electronic mail: osamura@chem.rikkyo.ac.jp

 © 2000 American Institute of Physics

Downloaded 08 May 2006 to 128.171.55.146. Redistribution subject to AIP license or copyright, see http://jcp.aip.org/jcp/copyright.jsp

TABLE I. Experimental beam conditions and 1σ errors: most probable velocity v_p, speed ratio S, most probable collision energy of the CN beam with the ethylene molecules, E_c, and center-of-mass angles, Θ_{CM}.

Experiment	v_p, m s^{-1}	S	E_c, kJ mol^{-1}	Θ_{CM}
CN/C_2H_4	1210±10	5.6±0.2	15.3±0.3	38.7±0.6
CN/C_2H_4	1520±10	4.5±0.2	21.0±0.4	32.5±0.3
C_2H_4	900±10	8.0±0.2	...	...

hydrocarbons are of great interest because of their relevance in combustion chemistry, gas lasers, astrochemistry, and solar system chemistry, with the most interesting case being the atmospheric chemistry of Saturn's moon Titan.[9,10] Because of that, chemical kinetics of CN reactions with the simplest olefins were extensively investigated down to temperatures as low as 25 K[11] demonstrating that these reactions have no entrance barrier. We have recently reported CMB studies on the reactions of CN($X\,^2\Sigma^+$) with (a) acetylene,[4] C_2H_2, (b) methylacetylene,[5] CH_3CCH, (c) benzene,[6] C_6H_6, and (d) dimethylacetylene,[7] CH_3CCCH_3; in all cases, the reactions were found to be dominated by a CN vs H exchange channel to form (a) cyanoacetylene, HCCCN, (b) methylcyanoacetylene, CH_3CCCN, and the cyanoallene isomer, $H_2CCCH(CN)$, (c) cyanobenzene, C_6H_5CN, (d) 1-cyano-1-methylallene, $CNCH_3CCCH_2$.

Here, we report our results on another interesting system, namely the reaction of cyano radicals with ethylene. Ethylene being present in the interstellar medium and Titan,[12] the title reaction is a good candidate to explain the formation of interstellar and planetary vinylcyanide, C_2H_3CN, via a CN vs H exchange. We have also performed *ab initio* molecular orbital calculations of the reaction potential energy surface in order to provide a global picture of the energy diagram. RRKM calculations have also been carried out to establish the main reaction pathway. Our results will be commented on in the contest of CN radical reactions with other unsaturated hydrocarbons; similarities and discrepancies with the strongly related reaction $F(^2P)+C_2H_4$ also studied in cross beam experiments[13] will be noted.

II. EXPERIMENT AND DATA ANALYSES

The experiments were performed by using the 35″ crossed molecular beam machine, which has been described elsewhere.[14] Briefly, a pulsed supersonic cyano radical beam, CN($X\,^2\Sigma^+;\nu=0$), in the vibrational ground state is generated *in situ* via laser ablation of graphite at 266 nm and subsequent reaction of the ablated species with neat nitrogen gas which acts also as seeding gas.[3] A Spectra Physics GCR 270-30 Nd-YAG laser operating at 30 Hz and 30 mJ per pulse was used for graphite ablation. A chopper wheel located after the ablation source and before the collision center selects a 9 μs segment of the CN beam; cf. Table I; the pulsed beam is made to intersect a second, pulsed ethylene, C_2H_4, beam at 90° in the interaction region. Reactively scattered species are detected using a triply differentially pumped detector consisting of a Brink-type electron-impact-ionizer, quadrupole mass filter, and a Daly ion detector.[15] Product velocity distributions were determined by measuring time-of-flight spectra (TOF) at different laboratory angles. Data accumulation times range up to 7 h at every angle. The laboratory angular distribution (LAB) is obtained by integrating TOF spectra at different laboratory angles and taking into account the cyano radical beam intensity drift. Quantitative information on the reaction dynamics is obtained by moving from the laboratory coordinate system to the center-of-mass (CM) one and analyzing the product angular, $T(\theta)$, and translational energy, $P(E_T)$, distributions into which the CM product flux can be factorized. The CM functions are actually derived by a forward convolution fit of the product laboratory angular and TOF distributions; the experimental resolution broadening (due to the TOF disk and detector slit sizes, disk velocity, ionizer length, and spread in beam velocities and angular divergences) is taken into account. The final outcome is the generation of a velocity flux contour map $I(\theta,u)$ in the center-of-mass frame, where the intensity is shown as a function of scattering angle θ and product speed u. This plot contains all the basic information of the reactive scattering process.

TABLE II. RRKM rate constants (s^{-1}) for the title reaction at two collision energies of 15.3 and 21.0 kJ mol^{-1}.

Collision energy, kJ mol^{-1}	15.3	21.0
$k_{\text{int 1}\rightarrow nc\text{-int 1}}$	2.77×10^5	6.97×10^5
$k_{\text{int 1}\leftarrow nc\text{-int 1}}$	6.87×10^7	1.55×10^8
$k_{\text{int 1}\rightarrow\text{int 2}}$	1.58×10^9	1.96×10^9
$k_{\text{int 1}\leftarrow\text{int 2}}$	6.57×10^8	8.47×10^8
$k_{\text{int 1}\rightarrow\text{int 3}}$	6.89×10^9	7.67×10^9
$k_{\text{int 1}\leftarrow\text{int 3}}$	8.56×10^{13}	8.74×10^{13}
$k_{\text{int 1}\rightarrow\text{int 4}}$	2.45×10^4	4.71×10^4
$k_{\text{int 1}\leftarrow\text{int 4}}$	9.10×10^{10}	1.37×10^{11}
$k_{\text{int 2}\rightarrow\text{int 5}}$	1.13×10^7	1.65×10^7
$k_{\text{int 2}\leftarrow\text{int 5}}$	1.39×10^{13}	1.49×10^{13}
$k_{\text{int 4}\rightarrow nc\text{-int 1}}$	1.75×10^{11}	2.61×10^{11}
$k_{\text{int 4}\leftarrow nc\text{-int 1}}$	1.17×10^7	1.99×10^7
$k_{nc\text{-int 2}\rightarrow nc\text{-int 1}}$	2.01×10^3	9.71×10^3
$k_{nc\text{-int 2}\leftarrow nc\text{-int 1}}$	8.49×10^4	3.82×10^5
$k_{\text{int 5}\rightarrow nc\text{-int 2}}$	2.95×10^{13}	3.05×10^{13}
$k_{\text{int 5}\leftarrow nc\text{-int 2}}$	3.38×10^8	4.42×10^8
$k_{nc\text{-int 1}\rightarrow nc\text{-products}}$	4.64×10^3	6.01×10^4
$k_{nc\text{-int 2}\rightarrow nc\text{-products}}$	1.85×10^4	2.94×10^5
$k_{\text{int 1}\rightarrow\text{products}}$	8.38×10^8	1.12×10^9
$k_{\text{int 2}\rightarrow\text{products}}$	4.06×10^9	5.41×10^9

III. ELECTRONIC STRUCTURE AND RRKM CALCULATIONS

The potential energy surface (PES) of the reaction between ethylene and the cyano radical has been examined in terms of *ab initio* molecular orbital methods. We have employed the hybrid density functional B3LYP method, i.e., Becke's three-parameter nonlocal exchange functional[16] with the correlation functional of Lee, Yang, and Parr,[17] and the 6-311G(d,p) basis set.[18] All computations have been carried out using the GAUSSIAN 98 program package.[19] The structures of the intermediates and transition states were confirmed with the vibrational analysis; all relative energies shown in this paper are the corrected values of the zero-point

Downloaded 08 May 2006 to 128.171.55.146. Redistribution subject to AIP license or copyright, see http://jcp.aip.org/jcp/copyright.jsp

vibrational energies. The coupled cluster CCSD(T) calculations with the 6-311G(d,p) basis set have also been performed for some of the critical structures in order to refine the energetics.[20]

According to the quasiequilibrium theory or RRKM theory,[21] the rate constant $k(E)$ at a collision energy E for a unimolecular reaction $A^* \rightarrow A^{\#} \rightarrow P$ can be expressed as

$$k(E) = \frac{\sigma}{h} \cdot \frac{W^{\#}(E-E^{\#})}{\rho(E)}, \quad (1)$$

where σ is the symmetry factor, $W^{\#}(E-E^{\#})$ denotes the total number of states of the transition state (activated complex) $A^{\#}$ with the barrier $E^{\#}$, $\rho(E)$ represents the density of states of the energized reactant molecule A^* and P is the product or products. The harmonic oscillator and rigid rotor approximation are assumed for the species involved throughout the rate constant calculations. The saddle point method is applied to evaluate $\rho(E)$ and $W(E)$. The rate equations for the reaction mechanism deducted from the *ab initio* potential energy surface are subsequently solved to obtain the branching ratios.

IV. RESULTS

A. Reactive scattering signal

Reaction products were detected at mass-to-charge ratio, m/e, of 53, 52, 51, 50 corresponding to the ions $C_3H_3N^+$, $C_3H_2N^+$, C_3HN^+, and C_3N^+; cf. Figs. 1–4. TOF spectra recorded at all m/e revealed identical patterns and could be fit with the same center-of-mass functions. This unambiguously indicates that the only detected product under our experimental conditions has a gross formula C_3H_3N and that it partly fragments to $C_3H_2N^+$, C_3HN^+, and C_3N^+ in the electron impact ionizer. No adduct was observed at $m/e=54$, indicating that under single collision conditions the initially formed adduct (see below) fragments because of its high energy content. Due to the high background signal at $m/e=27$, we were unable to detect reaction products from the possible H abstraction reaction giving HCN or HNC and vinyl radical, C_2H_3.

B. Laboratory angular distributions (LAB) and TOF spectra

Because of the best signal-to-noise ratio, the complete set of final measurements were carried out at $m/e=50$. We have performed scattering experiments at two different collision energies, E_c, of 15.3 and 21.0 kJ mol^{-1} (see Table II). Figures 1 and 2 report the laboratory product angular distributions together with the most probable Newton diagrams (showing the kinematics of the processes) at collision energies $E_c=15.3$ and 21.0 kJ mol^{-1}, respectively. Selected TOF spectra are shown in Figs. 3 and 4 for the lower (15.3 kJ mol^{-1}) and higher (21.0 kJ mol^{-1}) collision energy. The solid lines superimposed on the experimental results are the calculated curves when using the CM best-fit functions (see below). Both laboratory angular distributions peak very close to the CM position angles (38.7° and 32.5° for the lower and higher collision energy experiment, respectively) show about the same intensity in the backward and forward directions

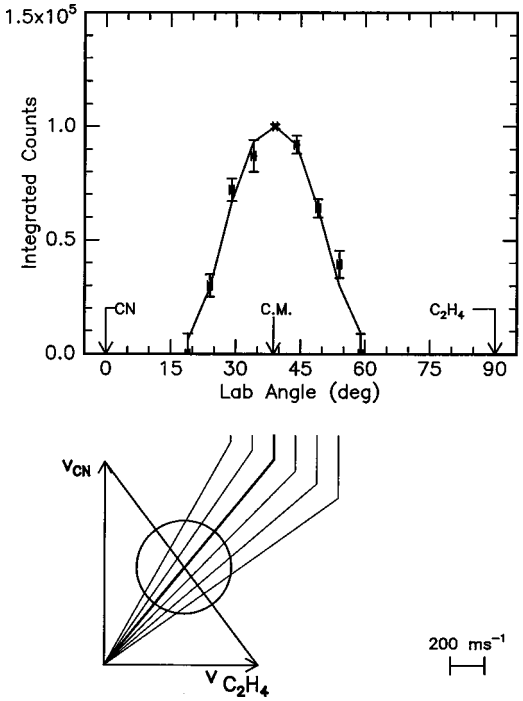

FIG. 1. Lower: Newton diagram for the reaction $CN(X\,^2\Sigma^+) + C_2H_4(X\,^1A_g) \rightarrow C_2H_3CN(X\,^1A') + H(^2S_{1/2})$ at a collision energy of 15.3 kJ mol^{-1}. The circle delimits the maximum center-of-mass recoil velocity of the C_2H_3CN product, assuming all the available energy is released as translational energy. Upper: Laboratory angular distribution of the C_3H_3N product. Circles and error bars indicate experimental data; the solid line the calculated distribution.

(with respect to the CN radical beam direction) and are quite broad with scattered products extending for about 45°. In both experiments, time-of-flight spectra taken in the range of angles close to the center-of-mass position angle show some structure with weak shoulders.

The limiting circles shown in Figs. 1 and 2 delimit the maximum center-of-mass recoil speed of the C_2H_3CN product when assuming that all the available energy is released as product translational energy. If we compare this limit with the experimentally determined scattering range of the C_3H_3N isomers, the substantial coincidence of the angular ranges indicates that the thermodynamically most stable radical product, vinylcyanide, C_2H_3CN, is mainly formed.

C. Center-of-mass translational energy distribution, $P(E_T)$

Experimental data were fit using one center-of-mass angular distribution and a single center-of-mass translational energy distribution; Figures 5 and 6 show the best-fit functions within the error limits. All $P(E_T)$ peak at about 20–25 kJ mol^{-1}. This suggests that the exit transition state from the decomposing intermediate to the products is likely to be tight and hence involves a repulsive bond rupture. Furthermore, the maximum translational energy of the $P(E_T)s$ is found to be 100–110 kJ mol^{-1} (Fig. 5) and 110–120 kJ mol^{-1} (Fig. 6). Extending or cutting both translational energy distributions by 10–15 kJ mol^{-1} has no influence on the fit. If we account for the relative collision energies of 15.3 and 21.0 kJ mol^{-1}, the CN/H exchange reaction is found to be exo-

Downloaded 08 May 2006 to 128.171.55.146. Redistribution subject to AIP license or copyright, see http://jcp.aip.org/jcp/copyright.jsp

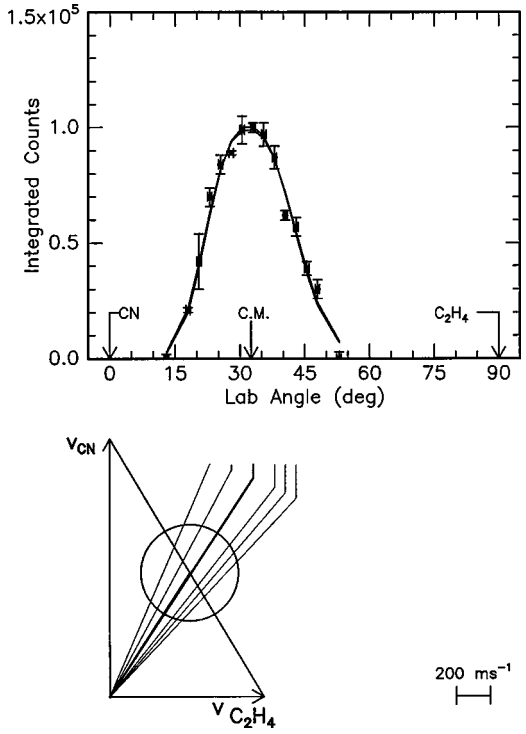

FIG. 2. Lower: L Newton diagram for the reaction $CN(X\,^2\Sigma^+)+C_2H_4(X\,^1A_g)\rightarrow C_2H_3CN(X\,^1A')+H(^2S_{1/2})$ at a collision energy of 21.0 kJ mol^{-1}. The circle delimits the maximum center-of-mass recoil velocity of the C_2H_3CN product, assuming all the available energy is released as translational energy. Upper: Laboratory angular distribution of the C_3H_3N product. Circles and error bars indicate experimental data, the solid line the calculated distribution.

thermic by about 90–100 kJ mol^{-1}. According to our electronic structure calculations (see below), the thermochemistry of the channel leading to vinylcyanide, C_2H_3CN, and $H(^2S)$ is quite different from that of the channel leading to isovinylcyanide, C_2H_3NC, isomer and $H(^2S)$, with an exothermicity of -95.0 kJ mol^{-1} in contrast to $+4.0$ kJ mol^{-1}.

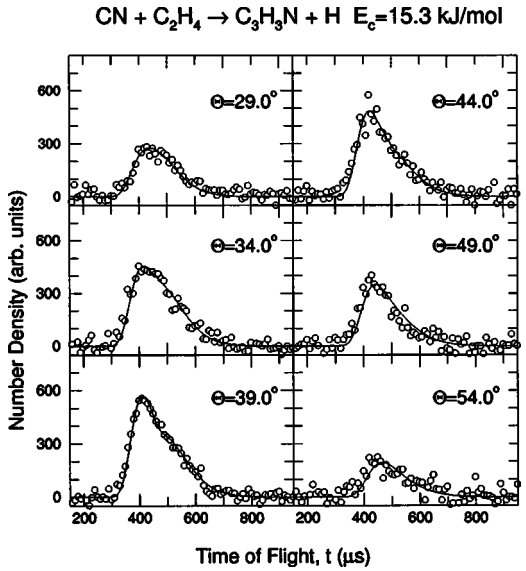

FIG. 3. Time-of-flight data of selected laboratory angles as indicated in Fig. 1. The dots indicate the experimental data; the solid lines, the calculated fit.

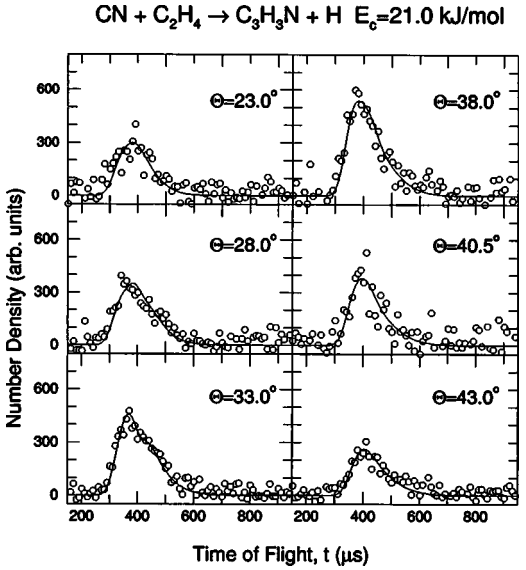

FIG. 4. Time-of-flight data of selected laboratory angles as indicated in Fig. 2. The dots indicate the experimental data, the solid lines, the calculated fit.

Therefore, based on the energy cutoff of the product translational distributions we can conclude that the thermodynamically more stable vinylcyanide isomer is mainly formed from the title reaction. Taking into account the exothermicity of

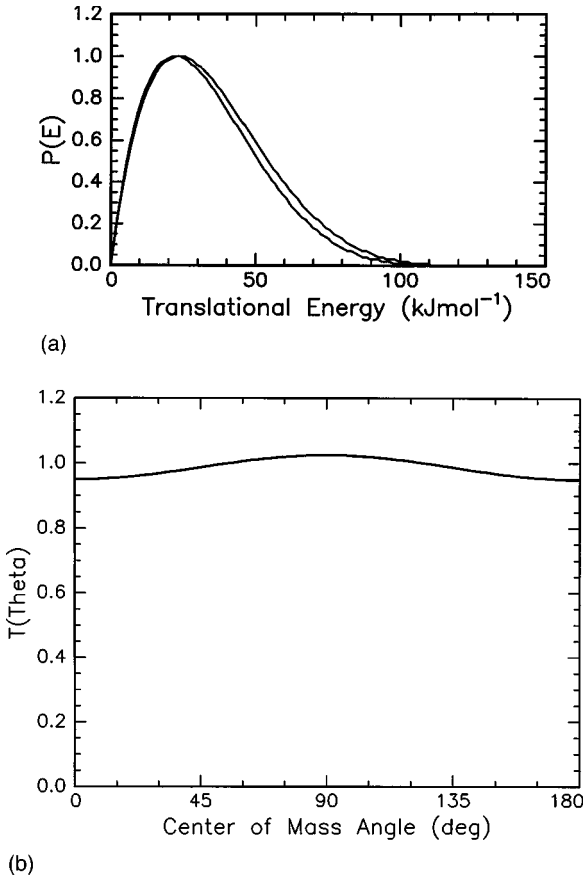

FIG. 5. Center-of-mass angular flux distribution (lower) and translational energy flux distribution (upper) for the reaction $CN(X\,^2\Sigma^+)+C_2H_4(X\,^1A_g)\rightarrow C_2H_3CN(X\,^1A')+H(^2S_{1/2})$ at a collision energy of 15.3 kJ mol^{-1}.

Downloaded 08 May 2006 to 128.171.55.146. Redistribution subject to AIP license or copyright, see http://jcp.aip.org/jcp/copyright.jsp

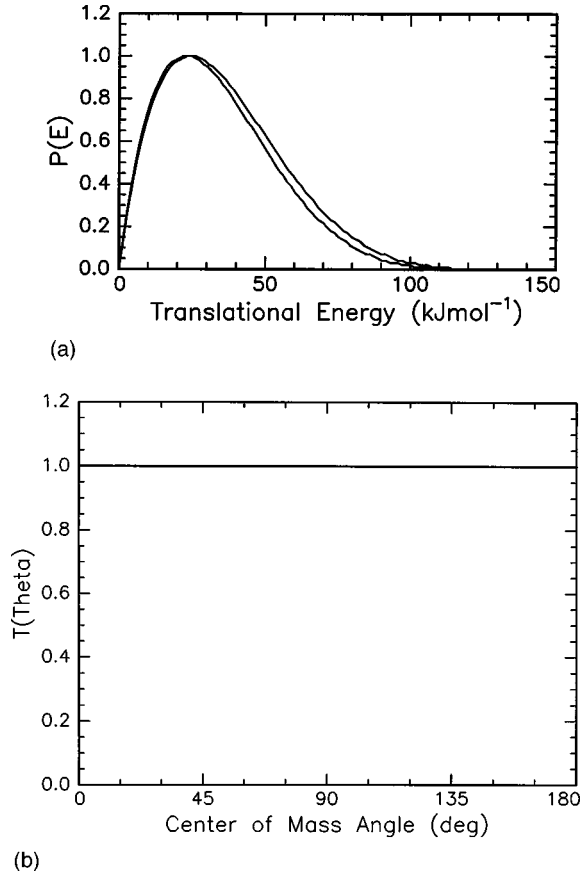

FIG. 6. Center-of-mass angular flux distribution (lower) and translational energy flux distribution (upper) for the reaction $CN(X\,^2\Sigma^+)+C_2H_4(X\,^1A_g)\rightarrow C_2H_3CN(X\,^1A')+H(^2S_{1/2})$ at a collision energy of 21.0 kJ mol^{-1}.

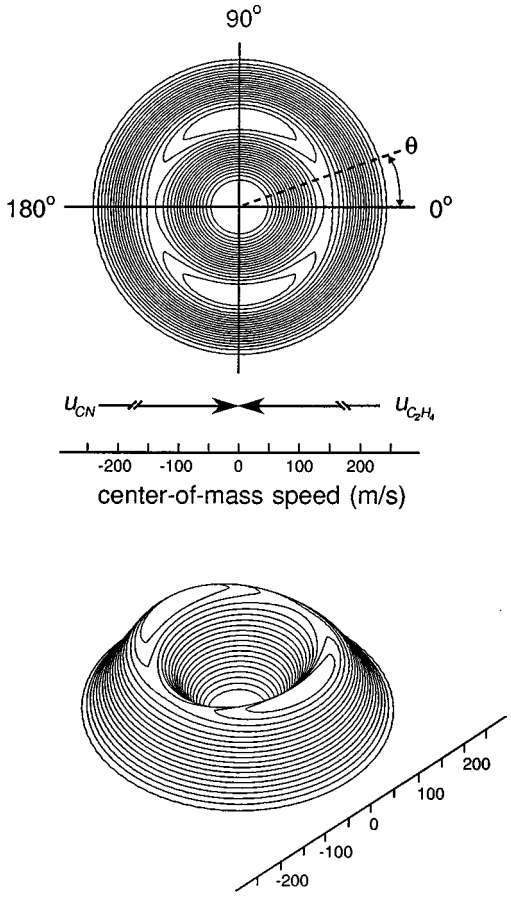

FIG. 7. Center-of-mass velocity contour flux map distribution for the reaction $CN(X\,^2\Sigma^+)+C_2H_4(X\,^1A_g)\rightarrow C_2H_3CN(X\,^1A')+H(^2S_{1/2})$ at a collision energy of 15.3 kJ mol^{-1}. Units are given in m s^{-1}.

the C_2H_3CN+H channel, the fraction of the total available energy channeled into the translational degrees of freedom of the products is about 30%–35%.

D. Center-of-mass angular distributions, $T(\theta)$, and flux contour maps, $I(\theta,u)$

At both collision energies, the $T(\theta)$ and $I(\theta,u)$ are forward–backward symmetric; cf. Figs. 5–8. This suggests that the reaction follows indirect scattering dynamics via complex formation. The observed 0°–180° symmetry may imply either a lifetime of the decomposing complex longer than its rotational period or a ''symmetric exit transition state.'' In the latter case, the rotation interconverts leaving hydrogen atoms in the decomposing complex via a proper rotation axis, and the complex fragments with equal probability along a direction defined by θ or π-θ; this behavior would result in a symmetric flux distribution although the lifetime of the complex might be less than a rotational period.[22] At lower collision energy, a best fit of our data was achieved with a $T(\theta)$ peaking slightly at 90° with an intensity ratio $I(0°)/I(90°)=0.9-0.95$. The ''sideways scattering'' suggests geometrical constraints in the decomposing C_2H_4CN intermediate that define a specific orientation of the H atom emission; cf. Sec. V. At higher collision energy, a flat distribution was observed (see Fig. 6); as a matter of fact, however, a very minor sideways scattering preference could quite satisfactorily fit our experimental data as well. That can be rationalized as follows. If we consider the reversed reaction, i.e., the addition of an H atom to the vinylcyanide molecule, an increase of collision energy allows a wider range of reactive impact parameters. In the same manner, an increase of the energy available to the decomposing complex and the transition state implies more internal excitation and translates into a less defined direction of the departing H, turning into a flat angular distribution.

V. DISCUSSION

A. *Ab initio* C_3H_4N potential energy surface

In the following section we report the results of the computational investigation of the interaction of the cyano radical, $CN(X\,^2\Sigma^+)$ with the ethylene molecule, $C_2H_4(X\,^1A_g)$. With the radical center localized on the $^2\Sigma^+$ orbital of the carbon atom, CN can attack the π orbital of the ethylene molecule without an entrance barrier leading to a deeply bound (232 kJ mol^{-1}) C_s symmetric 1-cyanoethyl-2 radical intermediate, CH_2CH_2CN (int1) on the $^2A'$ surface; cf. Figs. 9–10. Our calculations show that after the initial attack, the CH_2 group of the ethylene molecule rotates almost 90° dur-

Downloaded 08 May 2006 to 128.171.55.146. Redistribution subject to AIP license or copyright, see http://jcp.aip.org/jcp/copyright.jsp

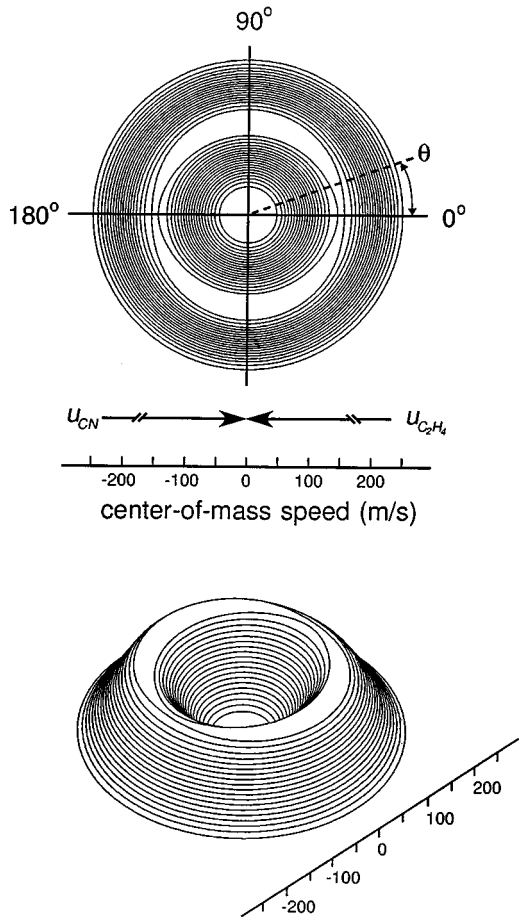

FIG. 8. Center-of-mass velocity contour flux map distribution for the reaction $CN(X\,^2\Sigma^+)+C_2H_4(X\,^1A_g)\rightarrow C_2H_3CN(X\,^1A')+H(^2S_{1/2})$ at a collision energy of 21.0 kJ mol^{-1}. Units are given in m s^{-1}.

ing the nonbarrier pathway to int1. An alternative pathway is the N-side attack of the CN radical to ethylene, Figs. 9 and 11. Since this reaction involves the lone-pair electrons on the nitrogen atom of the CN radical, we would expect that this reaction is energetically unfavorable. The potential energy surface, however, indicates attractiveness, and there is no transition state for the formation of a bound (-139 kJ mol^{-1}) 1-isocyanoethyl-2 radical, CH_2CH_2NC (nc-int1). The fact that the N-side attack to ethylene is barrierless shows a smooth electron delocalization of the unpaired electron from the carbon atom of the CN radical to the terminal carbon atom of the C_2H_4 moiety during the reaction pathway.

Both int1 and nc-int1 can isomerize via TS1a located only 11 kJ mol^{-1} below the energy of the separated reactants, Fig. 12. A lower-energy isomerization pathway involves a ring closure of int1 via TS4a to a tetracyclic C_3H_4N intermediate (-73 kJ mol^{-1}), which, in turn, ring opens via TS4b to nc-int1. Besides the cyano–isocyano isomerization, a ring closure in int1 forms a tricyclic intermediate via TS3 that resides in a shallow potential energy well only bound by 8 kJ mol^{-1}. In strong analogy to int1, nc-int1 can undergo ring closure as well to form a tricyclic nc-int3 intermediate via nc-TS3. However, nc-int3 is even more weakly bound (3 kJ mol^{-1}) than the corresponding int3 intermediate, and the transition state to ring closure/ring opening is located 35 kJ mol^{-1} above the energy of the separated reactants.

Here int1 and nc-int1 can either undergo both H atom elimination or hydrogen atom migration. The hydrogen fragmentation pathways follow tight exit transition states located 16 kJ mol^{-1} (TS1b) and 8 kJ mol^{-1} (nc-TS1b) above the products in an exothermic reaction of -95 kJ mol^{-1} (the formation of the C_2H_3CN isomer) and an endothermic reaction of $+4$ kJ mol^{-1} (the formation of the C_2H_3NC isomer). Both intermediates int1 and nc-int1 have an unpaired electron on the terminal carbon atom. Since the carbon–carbon bond of the ethylene moiety becomes a single bond, the CH_2 moieties of int1 and nc-int1 are freely rotating and their energies do not depend on the twisting angles of the C–C bond of an ethylene part. As the geometries of TS1b and nc-TS1b shown in Figs. 10 and 11, the structures of the transition states indicate that the hydrogen atom leaves almost perpendicular to the molecular plane of the product species, i.e., 105.4° (C_2H_3CN; dihedral angle H– – –C–C–H: 96.0°) and 102.8° (C_2H_3NC). Alternatively, the 1,2-H atom shifts in int1 and nc-int1 form intermediates int2 and nc-int2 that are stabilized by 286 and 192 kJ mol^{-1} with respect to the reactants. Int2 represents the global minimum of the C_3H_3N potential energy surface. These H atom shifts from the central carbon atom to the terminal carbon atom produce the methyl group and the allylic π conjugation. The structures of int2 and nc-int2 indicate a double bond character between the radical carbon and CN or NC group; cf. Figs. 10–11. A cyclic intermediate int5 connects isomers int2 and nc-int2 via transition states TS5a and TS5b; Fig. 13. The fate of int2 and nc-int2 is governed by a final carbon–hydrogen bond rupture via loose exit transition states TS2b and nc-TS2b. The structures of the transition states indicate that the C–H distances of the breaking bonds is more than 235 pm; furthermore, their geometries are very close to the product structures, and the H atom is emitted almost perpendicular to the molecular plane [106.0° (dihedral angle H– – –C–C–H: 90.5°) and 105.0°, respectively].

In addition to these energetically favorable reaction pathways, the C_3H_4N potential energy surface comprises high-energy isomers as well. We first examined the reactions of the tetracyclic isomer int4; cf. Figs. 14 and 15. The former ethylenic carbon–carbon in int4 can undergo carbon–carbon rupture via a conrotatory ring opening to form a chain isomer int6 that is 96 kJ mol^{-1} more stable than int4. Alternatively, int4 can rearrange to the tricyclic isomer int7. Although int6 and int7 are energetically favorable compared to int4, the involved isomerization barriers located 59 and 85 kJ mol^{-1} above the energy of the reactants cannot be passed, even at our maximum collision energy of 21.0 kJ mol^{-1}. Hence, both isomers cannot be formed in our experiments.

We calculated further the energetics, structures, and vibrational modes of all tetracyclic and tricyclic C_3H_3N isomers that can be formally derived from the heavy atom skeleton of int3, nc-int3, int4, and int5; cf. Figs. 15–17. In these figures, there is no energy minimum for the singlet spin state; all singlet species shown are first-order transition states and turn out to ring open to the most stable C_2H_3CN or C_2H_3NC structures. Since all reactions are strongly endothermic, these isomers are not relevant to our experiments, and we did not

Downloaded 08 May 2006 to 128.171.55.146. Redistribution subject to AIP license or copyright, see http://jcp.aip.org/jcp/copyright.jsp

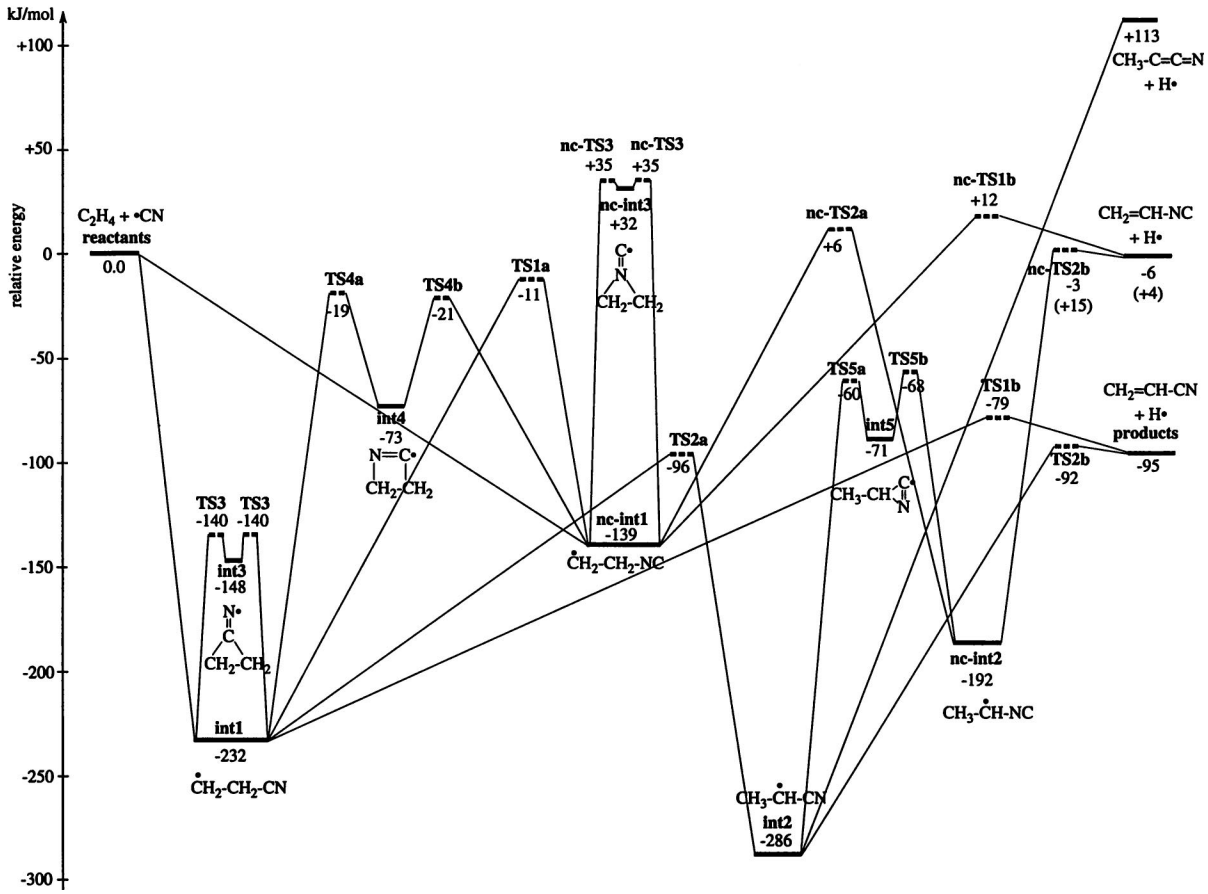

FIG. 9. Schematic representation of the C_3H_4N potential energy surface.

made an attempt to optimize the exit transition states to the triplet species. Further, a carbon–hydrogen bond rupture in int3 forms a triplet tricyclic isomer is a strongly endothermic reaction; Fig. 16. The C–H bond cleavage in nc-int3 gives no stable tricyclic isomer.

In addition, we have tackled potentially involved carbene reaction products. The notation of the carbene products is as follows: H atom loss from int1, int2, nc-int1, and nc-int2 corresponds to prod1, prod2, nc-prod1, and nc-prod2; the last digit 1 or 3 defines the singlet or triplet spin state. Besides the C–H bond rupture in int2 to form a cyanoethylene molecule, a hydrogen atom can be lost from the central carbon atom of int2 as well; cf. Fig. 18. This C–H bond scission produces a triplet methylene product CH_3–C–CN+H, which is 208 kJ mol^{-1} higher in energy than the most stable product cyanoethylene. Due to the stabilization of its π conjugation on the sp-hybridized CCN moiety, this carbene is quasilinear. The corresponding isocyanide methylene species triplet CH_3CNC is even 110 kJ mol^{-1} higher in energy. Both triplet carbenes that could be formed via H atom loss from int1 and nc-int1 are energetically not accessible in our experiments. These reactions are endothermic by 221 and 315 kJ mol^{-1}, respectively.

Finally, we have investigated also the interaction of the CN radical with the σ electron density of the ethylene molecule; cf. Fig. 19. If $CN(X\,^2\Sigma^+)$ approaches the hydrogen atom of ethylene in the molecular plane, hydrogen abstraction reaction takes place and produces HCN and vinyl radical $C_2H_3(X\,^2A')$. This potential energy surface is also attractive with the B3LYP calculation and the production of the HCN and C_2H_3 radical is shown to be 82 kJ mol^{-1} exothermic without an energy barrier. When the CN radical approaches the hydrogen atom of ethylene from the N side, we found a transition state (TS0b) for the hydrogen abstraction forming HNC and C_2H_3 located 22 kJ mol^{-1} above the energy of the reactants. The overall reaction is exothermic by 22 kJ mol^{-1}.

B. Reaction pathways

1. Energetical considerations

The high-energy cutoff of both $P(E_T)$'s is consistent with the formation of the thermodynamically most stable C_3H_3N isomer, i.e., vinylcyanide in its $^1A'$ electronic ground state. Our data suggest a reaction exothermicity of about 90–100 kJ mol^{-1}, whereas the electronic structure calculations reveal 95.0 kJ mol^{-1}. These data are in excellent agreement with recent thermodynamical data showing 90.0 kJ mol^{-1}.[23] Since the formation of isocyanoethylene is endothermic by 4.0 kJ mol^{-1}, this isomer can be likely excluded as a major contributor. This conclusion gains further support from the involved potential energy surface, cf. Figs. 9–11. C_2H_3NC formation, indeed, must proceed via nc-int2 or nc-int1. If nc-int1 is formed, it is expected to react preferentially through the lowest-energy barrier pathway via int4 to int1 or

Downloaded 08 May 2006 to 128.171.55.146. Redistribution subject to AIP license or copyright, see http://jcp.aip.org/jcp/copyright.jsp

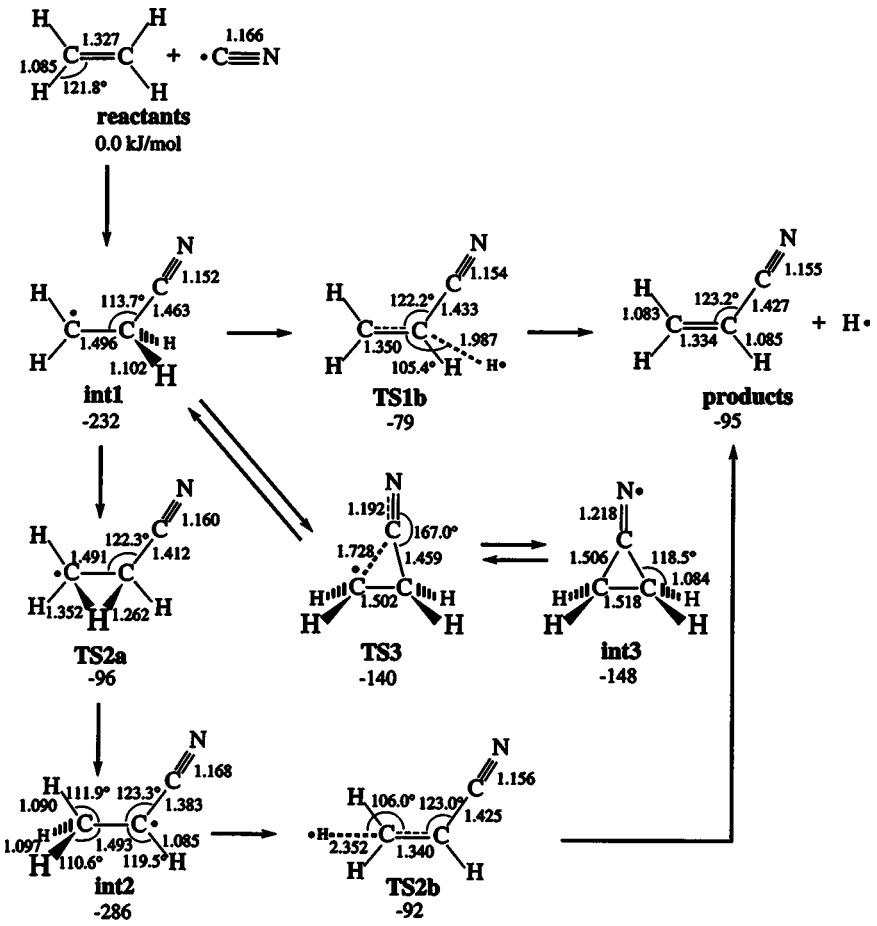

FIG. 10. Important bond distances in angstroms and bond angles in degrees of reactants, intermediates, and transition states involved in the formation of vinylcyanide.

a direct isomerization to int1. Even if a minor amount of nc-int1 undergoes a hydrogen shift via nc-TS2a to nc-int2, the latter does not evolve to the isocyanoethylene isomer, but follows the energetically more favorable pathway via int5 to int2. Therefore, none of the involved isocyano intermediates is expected to decompose to the C_2H_3NC isomer. Likewise, none of the carbene structures as shown in Fig. 18 is energetically accessible under our experimental conditions. Here, even the formation of thermodynamically most stable carbene, triplet 1-methyl-1-cyanocarbene, CH_3CCN, is too endothermic ($+113$ kJ mol^{-1}) considering our maximum collision energy of 21.0 kJ mol^{-1}. Reaction energies to the remaining triplet carbenes are highly endothermic and are calculated to be $+225$ kJ mol^{-1} (1-methyl-1-isocyanocarbene, CH_3CNC), $+221$ kJ mol^{-1} [$CH_2(CN)CH$], and $+315$ kJ mol^{-1} [$CH_2(NC)CH$]. Finally, none of the high-energy tetracyclic (Fig. 15) and tricyclic (Fig. 16) C_3H_3N isomers is energetically accessible. Therefore, we conclude that vinylcyanide is very likely the only C_3H_3N isomer as formed via a CN vs H atom exchange.

2. Consideration on the angular distribution

Based on our forward–backward symmetric flux contour map and the small fraction of 30%–35% of the total available energy channeled into the translational degrees of freedom, we can establish that the reaction proceeds through an indirect mechanism via the formation a complex having a lifetime longer than its rotation period. The only feasible complexes that can decompose into the experimentally detected vinylcyanide isomer are int1 and int2. A symmetric exit transition state is not involved because the decomposing intermediate(s) belong(s) to the C_s point group and shows no proper n-fold rotation axis.

3. RRKM rate constants and branching ratios

The branching ratios calculations employing the RRKM rate constants indicate that the vinylcyanide molecule is the only C_3H_3N isomer formed. Even if the CN radical reacts with the ethylene molecule to form the nc-int1 intermediate, a detailed investigation of the rate constants predicts a dominant isomerization to int4 ($k=1.17\times10^7$ s^{-1}) and int1 ($k=6.87\times10^7$ s^{-1}); int4 isomerizes back to nc-int1 ($k=1.75\times10^{11}$ s^{-1}). Both an alternative unimolecular decomposition of nc-int1 to C_2H_3NC+H or a rearrangement via nc-TS2a to nc-int2 have rate constants k less than about 8×10^4 s^{-1} and hence can be neglected. An alternative isomerization of int2 to nc-int2 followed by decomposition to C_2H_3NC can be ruled out as well. The ratios of the rate constants shows that the int2−int5 isomerization contributes less than 1%. Employing the stationary points int1, TS3, int3, TS2a, int2, TS5a, int5, TS5b, TS1b, nc-int2, TS2b, and C_2H_3CN+H, we calculated the branching ratios of a H atom loss from int1 via TS1b to the products versus the reaction sequence int1→TS2a→int2→TS2b→products. About 40% of all ini-

Downloaded 08 May 2006 to 128.171.55.146. Redistribution subject to AIP license or copyright, see http://jcp.aip.org/jcp/copyright.jsp

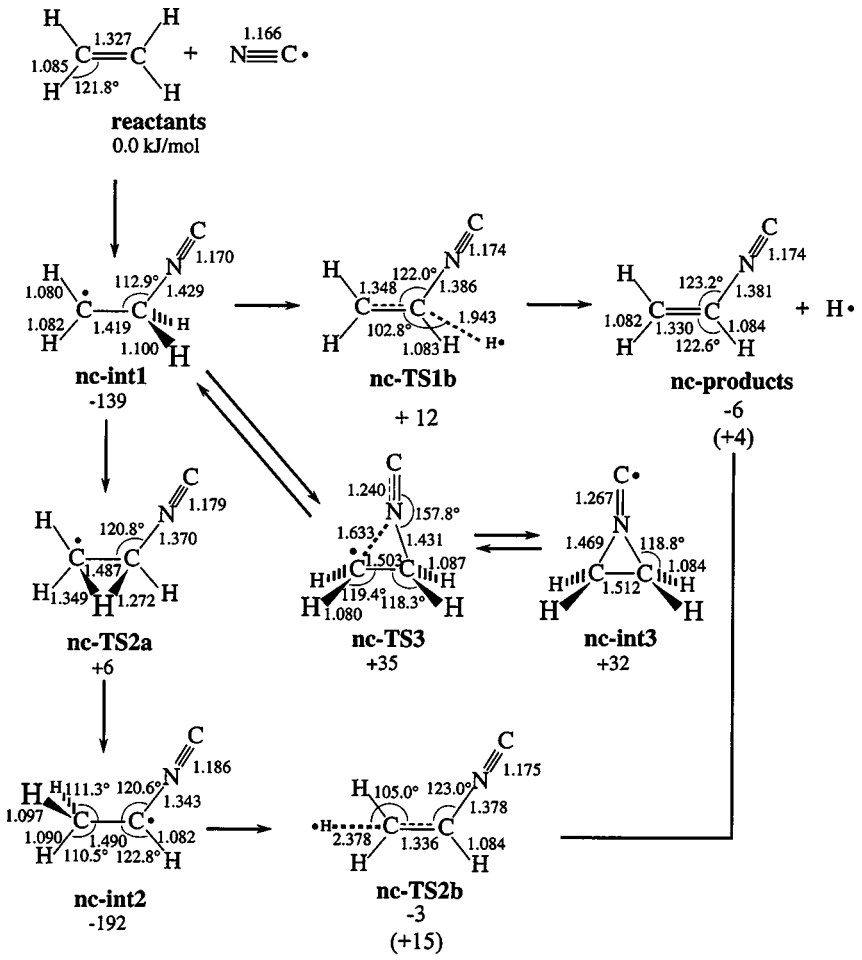

FIG. 11. Important bond distances in angstroms and bond angles in degrees of reactants, intermediates, and transition states involved in the formation of vinylisocyanide.

tially formed collision complexes int1 decompose to C_2H_3CN+H, whereas the remaining 60% undergo a 1,2 H shift to int2 prior to decomposition.

4. The actual reaction pathway

Our results indicate that the $CN(X\,^2\Sigma^+)$ radical attacks the π electron density in the highest occupied molecular orbital of the $C_2H_4(X\,^1A_g)$ molecule without an entrance barrier to form a carbon–carbon σ bond and a C_s symmetric 1-cyanoethyl-2 radical intermediate, CH_2CH_2CN (int1). The electronic structure calculations depict that after the initial attack, the CH_2 group of the ethylene molecule rotates almost 90° during the barrierless pathway to the CH_2CH_2CN complex. The CH_2CH_2CN intermediate is bound by 232 kJ mol^{-1} with respect to the reactants and resembles a prolate asymmetric top. The four heavy atoms are rotating nearly in plane perpendicular to the total angular momentum vector **J** around the *C* axis. The fate of int1 is twofold: branching ratios show that 40% of all 1-cyanoethyl-2 radical intermediates undergo C–H bond rupture via a tight exit

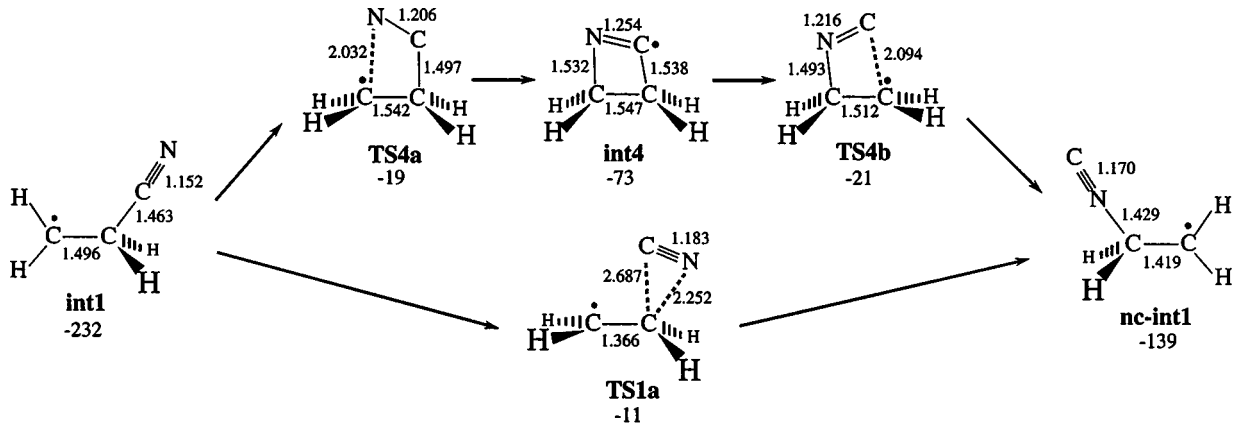

FIG. 12. Important bond distances in angstroms and bond angles in degrees of intermediates and transition states involved in the int1–nc-int1 isomerization.

Downloaded 08 May 2006 to 128.171.55.146. Redistribution subject to AIP license or copyright, see http://jcp.aip.org/jcp/copyright.jsp

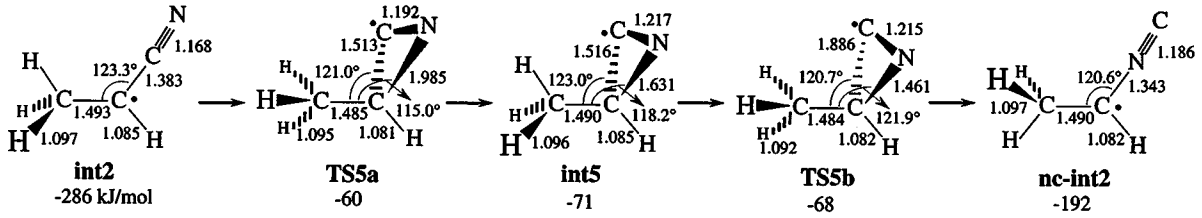

FIG. 13. Important bond distances in angstroms and bond angles in degrees of intermediates and transition states involved in the int2–nc-int2 isomerization.

transition state located 16 kJ mol^{-1} above the products (cf. Sec. V C for a detailed discussion) while the remaining 60% of int1 undergoes a 1,2 H atom shift to CH_3CHCN (int2) prior to a H atom release and the formation of vinylcyanide excited to C-like rotations. As documented by the mild sideways peaking in the CM angular distribution, the departing H atom is emitted almost parallel to the total angular momentum vector **J**. This is confirmed by the calculated geometry of exit transition states TS1b and TS2b, where the angles of the departing H atom are about 106° with respect to CCN plane and 96° with respect to CCH. Because of the low-frequency bending and wagging modes of 236, 303, 386, and 432 cm^{-1} (TS1b) and 150, 209, 242, and 383 cm^{-1} (TS2b), both transition states can result in a ''sideways'' peaking of the flux contour plot, i.e., the hydrogen atom is emitted almost parallel to the total angular momentum vector **J**. Although the geometry of the H atom emission is very similar in both transition states, TS2b is much looser compared to TS1b, showing imaginary frequencies of 285 and 741 cm^{-1}, respectively.

C. The exit transition states

When a long-lived complex is formed during a reaction, the resulting CM angular distribution $T(\theta)$ is forward–backward symmetric, i.e., the center-of-mass angular distribution is symmetric with respect to $\theta=\pi/2$.[24] The exact shape of the $T(\theta)$ is determined by the disposal of the total angular momentum **J**. In a typical crossed beam experiment, the reactant molecules undergo a supersonic expansion; a significant rotational cooling occurs, and the total angular momentum is predominantly given by the initial orbital angular momentum **L**. Since the products can be rotationally excited, Eq. (2) holds:

$$\mathbf{J}\approx\mathbf{L}\approx\mathbf{L}'+\mathbf{j}', \tag{2}$$

where $\mathbf{j}'$ is the rotational angular momentum of products and **L** and $\mathbf{L}'$ are the initial and final orbital angular momenta. The final recoil velocity vector, $\mathbf{v}'$, lies in a plane perpendicular to $\mathbf{L}'$ and, therefore, when the rotational excitation of products is significant, $\mathbf{v}'$ is not necessarily in a plane perpendicular to **J**. When $\mathbf{j}'$ is not zero, the probability distribution for the scattering angle θ, which is the center-of-mass angle between the initial relative velocity **v** and $\mathbf{v}'$, depends on the values of J, M, and M', where M and M' are the projections of **J** on the initial and final relative velocity, respectively. If the complex dissociates preferentially with low M' values, the final velocity $\mathbf{v}'$ is almost perpendicular to **J**, and therefore $\mathbf{v}'$ and **v** are almost parallel; in this case, the product intensity will be mainly confined to the poles, $\theta=0°$ and $\theta=180°$, similarly to the case of no product rota-

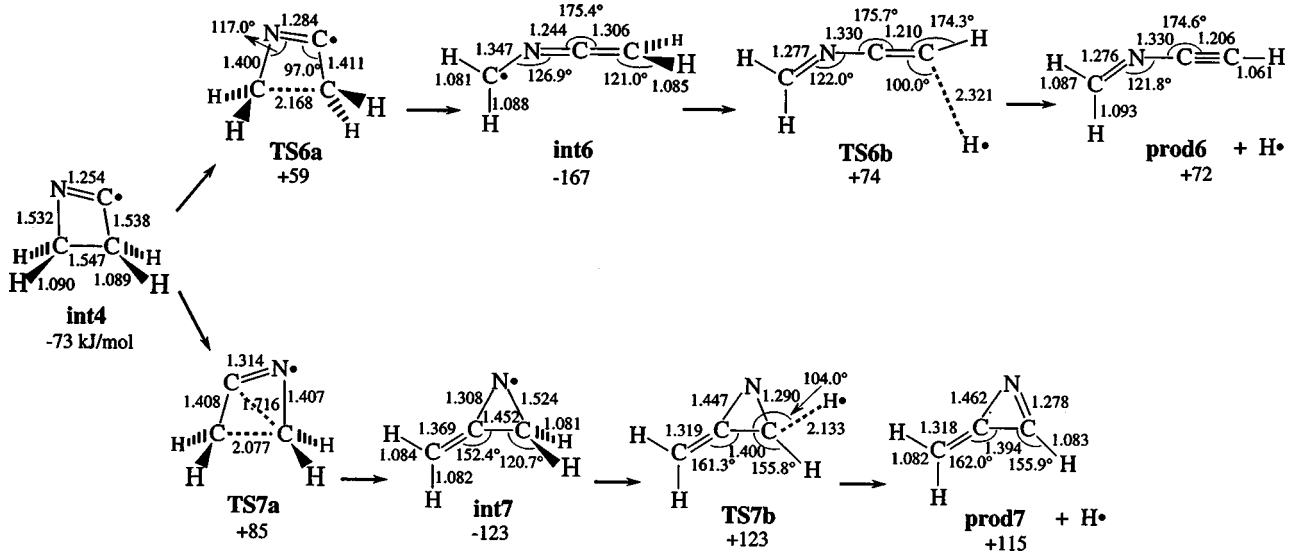

FIG. 14. Important bond distances in angstroms and bond angles in degrees of intermediates and transition states involved in the reaction of int4 to high-energy C_3H_3N isomers.

Downloaded 08 May 2006 to 128.171.55.146. Redistribution subject to AIP license or copyright, see http://jcp.aip.org/jcp/copyright.jsp

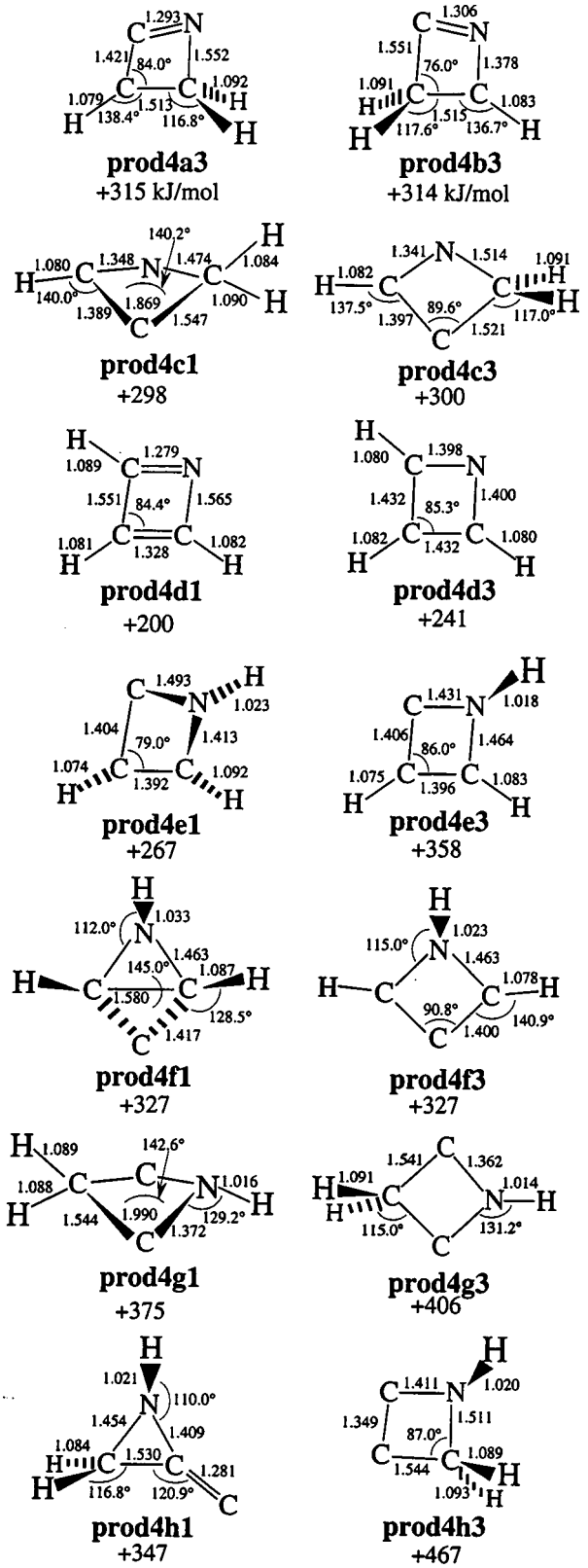

FIG. 15. Important bond distances in angstroms and bond angles in degree of high energy tetracyclic C_3H_3N isomers from int4.

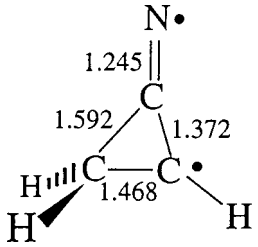

FIG. 16. Important bond distances in angstroms of high-energy tricyclic C_3H_3N isomers from int3.

tional excitation. However, when the collision complex dissociates mainly with high M' values, the final relative velocity will be almost parallel to **J** and perpendicular to **v** and the products will be preferentially scattered at $\theta = 90°$. Normally, a distribution of M' values is possible; in some cases, however, the geometry of the decomposing complex may imply a most probable M' value.

The best fit $T(\theta)$ of the lower collision energy experiment shows a symmetric shape and a peaking at $\theta = 90°$, suggesting that the H atom is ejected preferentially in a direction almost parallel to the total angular momentum vector. This finding is similar to the case of reaction $F + C_2H_4(C_2D_4) \rightarrow C_2H_3F(C_2D_3F) + H(D)$, studied in CMB experiments by Lee and co-workers in a wide range of collision energies;[13] also in this case a preference for sideways scattering was observed. We can say that in the title reaction, the calculated geometry of both relevant transition states TS1b and TS2b can well account for the observed sideways scattering properties. TS2b is very late, and hence the structure of the olefine part is very close to the product, so that the leaving H atom is in a position almost perpendicular to the double bond of the vinylcyanide product.

D. Comparison with the F/C_2H_4 system

Both the F atom and the CN radical attack barrierless the π electron density of the ethylene molecule to form a C_s symmetric $X–CH_2–CH_2$ radical intermediate ($X = F, CN$), which is stabilized in a deep potential energy well of $210\,kJ\,mol^{-1}$ ($X = F$) and $232\,kJ\,mol^{-1}$ ($X = CN$), respectively. All heavy atoms of the initial collision complex rotate almost in a plane roughly perpendicular to the total angular momentum vector **J**. Whereas Lee *et al.*[13] interpreted the CM angular distribution of the F/C_2H_4 system solely in terms of a long-lived $F–CH_2–CH_2$ complex emitting a light H atom almost parallel to **J**, the CN/C_2H_4 system suggests two microchannels. A recent investigation of the F/C_2H_4 system supports this finding: detailed electronic structure computations combined with RRKM calculations show that the 1,2 H shift in the initial $CH_2F–CH_2$ collision complex to CHF-CH_3 followed by C–H bond rupture in the methyl group does not

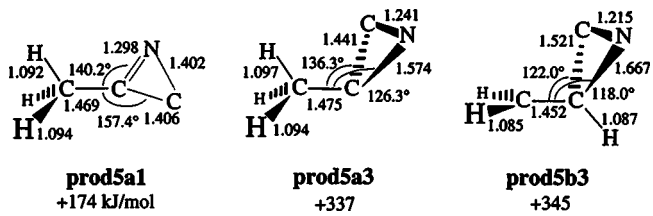

FIG. 17. Important bond distances in angstroms and bond angles in degrees of high-energy C_3H_3N isomers from int5.

Downloaded 08 May 2006 to 128.171.55.146. Redistribution subject to AIP license or copyright, see http://jcp.aip.org/jcp/copyright.jsp

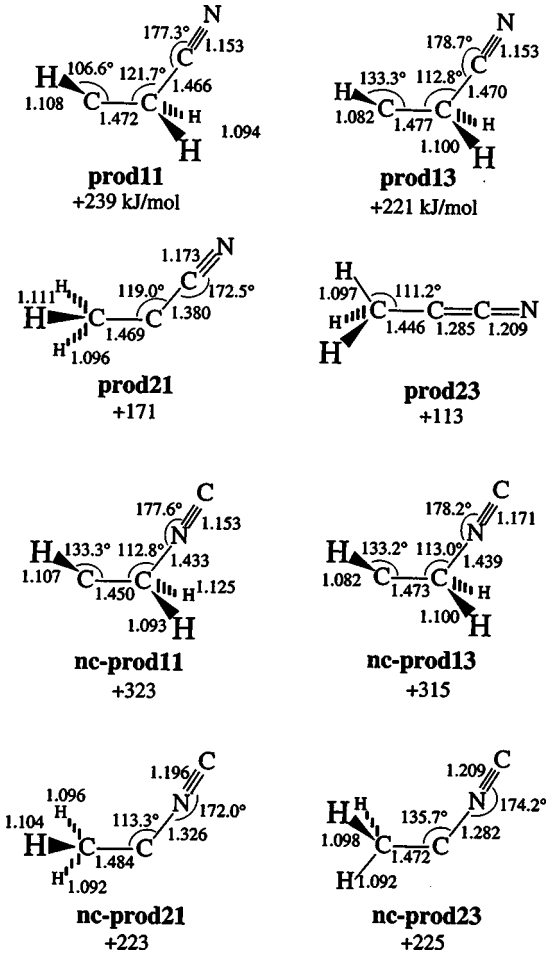

FIG. 18. Important bond distances in angstroms and bond angles in degrees of carbene reaction products.

significantly contribute to CH_2CHF formation.[25] In our title reaction, the channel one is in strong analogy to the F/C_2H_4 reaction and proceeds through the initial CH_2-CH_2-CN collision complex giving rise to a sideways peaking CM angular distribution. However, a second microchannel dominates the reaction dynamics and involves a 1, 2 H shift from the initial collision complex to $CH_3-CH-CN$ followed by H atom loss.

Despite the similarity in the angular distribution, the $P(E_T)$'s of the two systems show different characteristics. Whereas about 50% of the total available energy channels into translational energy of the C_2H_3F+H products, only 30%–35% go into the kinetic energy of the C_2H_3CN+H species. This enhanced fraction of internal energy is likely the result of the lower bending modes of the decomposing intermediates in the reaction of the cyano radical with the ethylene molecule and the transition states as compared to the F/C_2H_4 system. Further, the additional atom increases the vibrational degrees of freedom by 3; this might result in an enhanced internal energy compared to the $F+C_2H_4$ reaction. Finally, we would like to stress that the existence of a cyclic intermediate int3 is the most significant difference in the F/C_2H_4 and CN/C_2H_4 systems. Although int3 cannot play an active role in the chemistry of the C_3H_3N potential energy surface, the existence of int3 might increase the lifetime of int1 and hence the fraction of total available energy channeling into the internal degrees of freedom in the CN/C_2H_4 reaction compared to the F/C_2H_4 system.

VI. IMPLICATIONS TO INTERSTELLAR AND SOLAR SYSTEM CHEMISTRY

Our crossed beam approach combined with electronic structure calculations is the first explicit verification that C_2H_3CN can be formed via a neutral–neutral reaction between a cyano radical, CN ($X\,^2\Sigma^+$), and an ethylene molecule C_2H_4 ($X\,^1A_g$). Since the reaction has no entrance barrier, is exothermic, and all involved transition states are located well below the energy of the separated reactants, vinylcyanide can be even formed in very low-temperature extraterrestrial environments such as cold molecular clouds (10 K average translational temperature) and the atmosphere of Saturn's moon Titan. In both interstellar and planetary environments, the CN radical is ubiquitous, as found in the Taurus Molecular Cloud 1 (TMC-1), Orion Molecular Cloud (OMC-1), and outflow of old, dying carbon stars such as IRC-10126,[26] and upon collision with ethylene, a vinylcyanide molecule can be formed as detected, for example, toward Orion-KL[26] and SgrB2(N).[27] Based on our results, the C_2H_3NC isomer is predicted not to be formed. This is in line with astronomical observations since only C_2H_3CN was de-

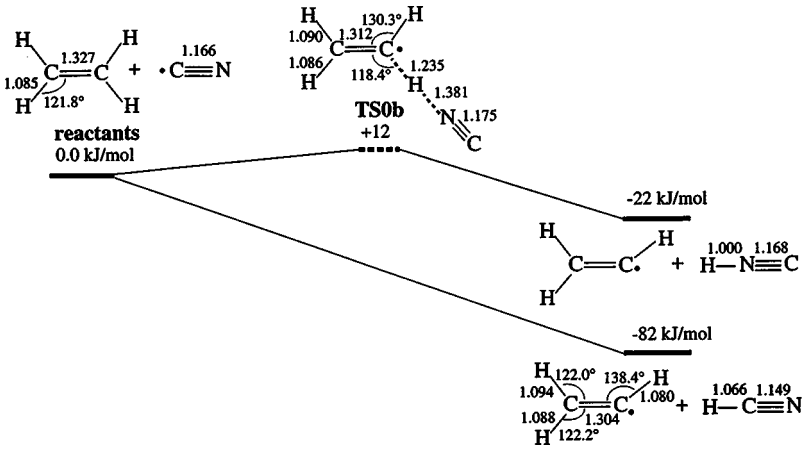

FIG. 19. Important bond distances in angstroms and bond angles in degrees of H atom abstraction channels to HCN and HNC.

Downloaded 08 May 2006 to 128.171.55.146. Redistribution subject to AIP license or copyright, see http://jcp.aip.org/jcp/copyright.jsp

tected. In high-temperature scenarios such as the outflow of carbon stars and combustion flames, synthesis of the isovinylcyanide isomer might proceed as well; this pathway is subject to further studies. Although the involved reaction intermediates CH_2CH_2CN and CH_3CHCN play no role in interstellar chemistry since their lifetime is too short to allow a third body stabilization, both doublet radicals must be included into chemical models of denser extraterrestrial environments such as Titan's atmosphere. In this denser atmosphere ternary encounters can divert the excess energy of the radicals to stabilize them.

VII. CONCLUSIONS

Our crossed molecular beam experiments combined with electronic structure calculations and RRKM studies show that the neutral–neutral reaction of the cyano radical, CN $(X\,^2\Sigma^+)$, with ethylene, C_2H_4 $(X\,^1A_g)$, is dominated by long-range dispersion forces. The reaction has no entrance barrier and is initiated by an attack of the CN radical with the carbon atom to the π electron density of the ethylene molecule to form a C_s symmetric 1-cyanoethyl-2 radical intermediate. The CH_2CH_2CN intermediate is bound by 232 kJ mol^{-1} with respect to the reactants and resembles a prolate asymmetric top. The four heavy atoms are rotating nearly in plane perpendicular to the total angular momentum vector **J** around the *C* axis. About 40% of all 1-cyanoethyl-2 radical intermediates shows C–H bond rupture via a tight exit transitions state located 16 kJ mol^{-1} above the products. The remaining 60% of the collision complex undergoes a 1,2 H atom shift to CH_3CHCN prior to a H atom release and the formation of vinylcyanide. Both decomposing complexes have lifetimes longer than its rotational period. As documented by the mildly sideways-peaked center-of-mass angular distribution and geometry of exit transition states, the H atom is emitted almost parallel to the total angular momentum vector **J**. The identification of the vinylcyanide strongly supports the inclusion of the title reaction in reaction networks modeling the chemistry in dark, molecular clouds, outflow of dying carbon stars, hot molecular cores, as well as the atmosphere of hydrocarbon-rich planets and hydrocarbon-rich satellites such as Saturn's moon Titan.

ACKNOWLEDGMENTS

R.I.K is indebted the Deutsche Forschungsgemeinschaft (DFG) for a Habilitation fellowship (IIC1-Ka1081/3-1). The work was further supported by Academia Sinica and the Taiwanese Petrol Organization. Most of the *ab initio* calculations were carried out at the computer center of the Institute for Molecular Science, Japan. This work was performed within the International Astrophysics Network, (http://po.iams.sinica.edu.tw/~kaiser/network.htm).

[1] For recent reviews see: P. Casavecchia, Rep. Prog. Phys. **63**, 355 (2000); P. Casavecchia, N. Balucani, and G. G. Volpi, Annu. Rev. Phys. Chem. **50**, 347 (1999).
[2] J. C. Whitehead, Rep. Prog. Phys. **59**, 993 (1996); K. Liu, R. G. MacDonald, and A. F. Wagner, Int. Rev. Phys. Chem. **9**, 187 (1990).
[3] R. I. Kaiser, J. Ting, L. C. L. Huang, N. Balucani, O. Asvany, Y. T. Lee, H. Chan, D. Stranges, and D. Gee, Rev. Sci. Instrum. **70**, 4185 (1999).
[4] L. C. L. Huang, Y. T. Lee, and R. I. Kaiser, J. Chem. Phys. **110**, 7119 (1999).
[5] L. C. L. Huang, N. Balucani, Y. T. Lee, R. I. Kaiser, and Y. Osamura, J. Chem. Phys. **111**, 2857 (1999).
[6] N. Balucani, O. Asvany, A. H. H. Chang, S. H. Lin, Y. T. Lee, R. I. Kaiser, H. F. Bettinger, P. v. R. Schleyer, and H. F. Schaefer III, J. Chem. Phys. **111**, 7457 (1999).
[7] N. Balucani, O. Asvany, A. H. H. Chang, S. H. Lin, Y. T. Lee, R. I. Kaiser, H. F. Bettinger, P. v. R. Schleyer, and H. F. Schaefer III, J. Chem. Phys. **111**, 7472 (1999).
[8] G. Scoles, *Atomic and Molecular Beam Methods* (New York University Press, New York, 1988), Vol. 1.
[9] D. W. Clarke and J. P. Ferris, ''Origins of life and evolution of the biosphere 27,'' 1997, p. 225; ESA Special Publication SP-338, 1992, Symposium on Titan.
[10] F. Raulin *et al.*, Adv. Space Res. **22**, 353 (1998).
[11] I. W. M. Smith, I. R. Sims, and B. R. Rowe, Chem. Eur. J. **3**, 1925 (1997).
[12] *Molecules in Interstellar Environments*, edited by E. F. van Dishoeck (Kluwer, Dordrecht, 1997).
[13] G. N. Robinson, R. E. Continetti, and Y. T. Lee, J. Chem. Phys. **92**, 275 (1990); J. M. Farrar and Y. T. Lee, *ibid.* **65**, 1414 (1976); J. M. Parson, K. Shobatake, Y. T. Lee, and S. A. Rice, Faraday Discuss. Chem. Soc. **55**, 344 (1973).
[14] Y. T. Lee, J. D. McDonald, P. R. LeBreton, and D. R. Herschbach, Rev. Sci. Instrum. **40**, 1402 (1969); R. I. Kaiser *et al.*, J. Chem. Phys. (in press).
[15] G. O. Brink, Rev. Sci. Instrum. **37**, 857 (1966); N. R. Daly, *ibid.* **31**, 264 (1960).
[16] A. D. Becke, J. Chem. Phys. **97**, 9173 (1992).
[17] C. Lee, W. Yang, and R. G. Parr, Phys. Rev. B **37**, 785 (1988).
[18] R. Krishnan, M. Frisch, and J. A. Pople, J. Chem. Phys. **72**, 4244 (1988).
[19] M. J. Frisch, G. W. Trucks, H. B. Schlegel *et al.*, GAUSSIAN 98, Revision D.4, Gaussian, Inc., Pittsburgh, PA, 1998.
[20] G. D. Purvis and R. J. Bartlett, J. Chem. Phys. **76**, 1910 (1982).
[21] H. Eyring, S. H. Lin, and S. M. Lin, *Basis Chemical Kinetics* (Wiley, New York, 1980).
[22] R. I. Kaiser, C. Ochsenfeld, M. Head-Gordon, and Y. T. Lee, Science **274**, 1508 (1996).
[23] NIST database http://webbook.nist.gov/.
[24] W. B. Miller, S. A. Safron, and D. R. Herschbach, Faraday Discuss. Chem. Soc. **44**, 108 (1967).
[25] K. Bolton, H. B. Schlegel, W. L. Hase, and K. Song, PCCP **1**, 999 (1999).
[26] P. Schilke *et al.*, Astrophys. J., Suppl. Ser. **108**, 301 (1997).
[27] A. Nummelin and P. Bergman, Astron. Astrophys. **341**, L59 (1999).

Downloaded 08 May 2006 to 128.171.55.146. Redistribution subject to AIP license or copyright, see http://jcp.aip.org/jcp/copyright.jsp